

## NOVEL PALLADIUM(II) COMPLEX DERIVED FROM MIXED LIGANDS OF DITHIZONE AND TRIPHENYLPHOSPHINE SYNTHESIS, CHARACTERIZATION, CRYSTAL STRUCTURE, AND DFT STUDY

Hikmat A. Mohamad<sup>1\*</sup>, Karwan O. Ali<sup>2</sup>, Thomas A. Gerber<sup>3</sup> and Eric C. Hosten<sup>3</sup>

<sup>1</sup>Department of Chemistry, College of Education, University of Salahaddin, Erbil 44001, Iraq

<sup>2</sup>Department of Physics, College of Science, University of Halabja, Halabja 46018, Iraq

<sup>3</sup>Department of Chemistry, Faculty of Science, Nelson Mandela University, Port Elizabeth 6031, South Africa

Received May 13, 2022; Revised June 8, 2022; Accepted June 8, 2022

**ABSTRACT.** A novel distorted square-planar palladium(II) complex of the type  $[Pd(Hdz)(PPh_3)Cl]$ , where (Hdz = dithizone mono deprotonate and  $PPh_3$  = triphenylphosphine), was synthesized in dichloromethane reactions between  $PdCl_2$  and a mixture of Hdz and  $PPh_3$ . The new Pd(II) complex has been identified by FT-IR, electronic spectra, DFT calculations, molar conductivity, and single-crystal X-ray diffraction. An X-ray diffraction study revealed the structure of this complex, indicating distorted square planar coordination geometry around the Pd(II) ion by N, S, P, and Cl donor atoms. XRD analysis has also shown that the Pd(II) complex contains one five-membered ring formed by the coordination of the Hdz ligand through the nitrogen and sulfur atoms to the palladium metal center. To comprehend the strength of nucleophilic and electrophilic attack between the ligands and metal ions, the natural bond orbital (NBO) was used. Finally, density functional theory (DFT) was used to show the molecular reactivity and stability of the ligands and palladium complex.

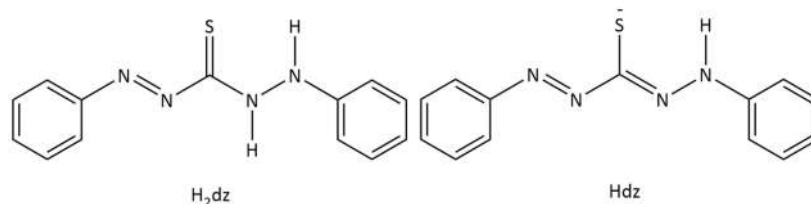
**KEY WORDS:** Palladium(II), Dithizone mono deprotonated, Distorted square planar geometry, NBO analysis, DFT calculations

### INTRODUCTION

Most divalent and trivalent transition metal ions form a colored complex with dithizone, which is a monoprotic organic acid capable of donating a proton and forming dithizonate [1]. The colored dithizone complexes have become an important reagent for the determination of trace elements [2]. Dithizone has been identified as a selective mercury adsorbent in industrial wastewater as well as a potential anticancer copper chelator [3, 4]. One comparative study showed that dithizone ( $H_2dz$ ) has diverse chelating forms, but the most common is monoanionic (Hdz) [5]. This monoanionic species is formed by deprotonation of the hydrazine N-H group (Scheme 1), followed by coordination of the sulfur atom and the terminal nitrogen atom of diazine to the metal ion. Furthermore, different coordination complexes of the monoanionic ligand (Hdz) in square-planar and octahedral geometries  $[M(Hdz)_2]$ ,  $M = Zn(II)$ ,  $Cd(II)$ ,  $Pt(II)$ , and  $Hg(II)$  have been prepared and characterized [6]. The monoanionic species (Hdz) can form neutral complexes of the formula  $[M(Hdz)_2]$  and  $[M(Hdz)_3]$  with multivalent metal ions such as  $Cu(II)$ ,  $Ni(II)$ ,  $Zn(II)$ ,  $Pd(II)$ ,  $Pt(II)$ ,  $Bi(III)$ , and  $Sn(IV)$ , as has been reported of the scientific literature [7-9]. This paper presents the results and discussion of the synthesis and characterization of the obtained complex  $[Pd(Hdz)(PPh_3)Cl]$  (using UV-Vis spectra, X-ray structural, FT-IR, and molar conductivity techniques). Theoretical studies, including Frontier Molecular Orbitals and Neutral bond orbitals (NBO), are achieved using density functional theory (DFT).

\*Corresponding author. E-mail: hikmat.mohamad@su.edu.krd

This work is licensed under the Creative Commons Attribution 4.0 International License



Scheme 1. The neutral dithizone is labeled as (H<sub>2</sub>dz) and the mono-deprotonated form as (Hdz).

## EXPERIMENTAL

### Materials and methods

PdCl<sub>2</sub> (99.9%), dithizone (99%), triphenylphosphine (98%), methanol (99.9%), dimethyl sulfoxide (99.8%), and dichloromethane (99.8%) were bought from Sigma Aldrich Company and used directly without further purification for the synthesis and analytical analysis of the complex. Crystallographic data for the complex was received on a Bruker Kappa Apex-II diffractometer with a radiation wavelength of ( $\lambda = 0.71073 \text{ \AA}$ ) and temperature of 200 K. FT-IR spectra were recorded using KBr discs on a Shimadzu FT-IR-8400S spectrophotometer in the wavenumber range of 4000–400 cm<sup>-1</sup>. The UV–Vis spectra of the free ligands and their complex were obtained in the DMSO solvent with a concentration of (10<sup>-3</sup> M) using an LTD Shimadzu spectrophotometer (AEUV1609 (UK) CO.) with a 1 cm quartz cell in the range of 200–800 nm. The molar conductivity analysis of the metal complex in DMSO (10<sup>-3</sup> M) at 25 °C was measured using a Meter CON 700 Benchtop conductivity meter. The melting point was determined using a scientific Stuart SMP3 melting point instrument.

### Synthesis of [Pd(Hdz)(PPh<sub>3</sub>)Cl]

To a homogenous mixture of dithizone (217 mg, 0.846 mmol) and PPh<sub>3</sub> (222 mg, 0.846 mmol) in CH<sub>3</sub>OH (25 mL), an equivalent solution of PdCl<sub>2</sub> (150 mg, 0.846 mmol) in CH<sub>3</sub>OH (25 mL) was added dropwise. The solution was further refluxed for 2 h at 55 °C with a formation of a red-brown precipitate, which was separated by filtration and dried at room temperature. After two weeks of slow evaporation of a dichloromethane solution, the red-brown crystals of the type [Pd(Hdz)(PPh<sub>3</sub>)Cl] complex were obtained. m.p. 82–84 °C. Yield: 558 mg (94.7 %). FT-IR (KBr, cm<sup>-1</sup>): 3400 (*m*), 3055 (*w*), 1579 (*m*), 1481 (*m*), 1436 (*s*), 1307 (*w*), 750 (*w*), 694 (*s*).

### X-Ray crystallography

Slow evaporation of the dichloromethane solution yielded red-brown crystals of the complex after two weeks. The crystal data were collected on a Bruker Kappa Apex II diffractometer using smart software at a low temperature (200 K) with graphite monochromatic Mo K radiation wavelength (0.071 073 nm). The structure was solved with SHELXT-2018/2 using a dual-space algorithm and refined by least-squares procedures using SHELXL-2018/3 as a graphical interface [10, 11]. C, P, N, Cl, S, and Pd atoms were refined on F<sup>2</sup> anisotropic parameters. The hydrogen atoms on nitrogen and carbon atoms were created geometrically and refined isotropically [12]. The crystal data and structure refinement details are listed in Table 1.

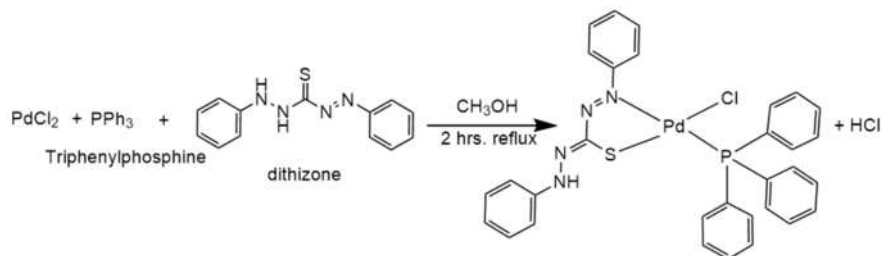
Table 1. Crystal and structure refinement data of the complex.

CCDC number	2133589
Empirical formula	C <sub>31</sub> H <sub>26</sub> ClN <sub>4</sub> PPdS
Formula weight	659.44
Temperature, K	200
Wavelength, nm	0.71073
Crystal system	monoclinic
Space group	<i>P</i> 21/ <i>c</i>
Crystal size, mm	0.09 x 0.25 x 0.40
<i>a</i> /Å	12.7599 (9)
<i>b</i> /Å	16.8093 (10)
<i>c</i> /Å	14.5886 (10)
$\alpha$ /°	90
$\beta$ /°	114.082 (3)
$\gamma$ /°	90
<i>V</i> /Å <sup>3</sup>	2856.7 (3)
<i>Z</i>	4
<i>D<sub>c</sub></i> /g cm <sup>-3</sup>	1.533
Absorption coefficient, mm <sup>-1</sup>	0.900
$\theta$ range for data collection, °	1.7, 28.3
Dataset	-17:17; -14:22; -19:19
<i>F</i> <sub>000</sub>	1336
No. of reflections	7071
No. of parameters	356
<i>R</i> <sub>int</sub>	0.038
<i>R</i> <sub>1</sub> , <i>wR</i> <sub>2</sub>	0.0277, 0.0592
<i>S</i>	1.02
[ <i>I</i> > 2σ( <i>I</i> )]	5557
Δρ <sub>min</sub> , Δρ <sub>max</sub> /eÅ <sup>-3</sup>	-0.44, 0.37

### Computational details

The theoretical calculation was performed with the Gaussian 09 software package. The frontier molecular orbitals of ligands and the Pd(II) complex were represented using density functional theory (DFT) with the B3LYP hybrid level at the LanL2Dz basis set [13, 14]. The neutral bond orbital (NBO) analysis of the compounds was achieved using the Gaussian 09 program at the B3LYP/LanL2Dz level of theory [15].

## RESULTS AND DISCUSSION



Scheme 2. The synthesis method of the target complex.

*Synthesis of complex*

The synthesis of the Pd(II) complex is illustrated in Scheme 2. The desired complex of the type [Pd(Hdz)(PPh<sub>3</sub>)Cl], where (Hdz = dithizone mono-deprotonate and PPh<sub>3</sub> = triphenylphosphine), was synthesized in dichloromethane at room temperature by reactions between PdCl<sub>2</sub> and a mixture of dithizone and triphenylphosphine in a molar ratio of 1:1:1. The Pd(II) complex was produced in high yield as red-brown crystals suitable for X-ray crystallography analysis.

*Single X-ray crystallography study*

To better understand the coordination geometry around the Pd(II) metal, X-ray diffraction studies were used to identify the complex's typical molecular geometry. Red-brown crystals, suitable for X-ray diffraction analysis, were grown by slow evaporation of a dichloromethane solution. The geometrical structure of the complex and atom numbering scheme is shown in (Figure 1). Relevant bond angles and bond distances for the unit cell are collected in Table 2. (Figure 1) depicts the Pd(II) metal center in a distorted square planar geometry, bonded by the P atom of the PPh<sub>3</sub> ligand and two dithizone ligand atoms (N and S) that form a five-membered ring. The Pd atom lies 0.1207(5) Å above the least square plane formed by the atoms N1, S1, P1, and C11. This Pd(II) complex is monoclinic and crystallizes in the space group P2<sub>1</sub>c with Z = 4. The angles between neighboring atoms of this Pd(II) complex are near to the ideal square planar value of 90°, with the C11-Pd1-N1 [98.05(5)°], S1-Pd1-P1 [87.85(2)°], and the largest deviations were observed for S1-Pd1-N1 [82.65(5)°] angle [16]. The Pd1-C11, Pd1-S1, Pd1-P1, and Pd1-N1 bond distances in the complex are in the ranges 2.3453(6), 2.2669(6), 2.2539(6), and 2.1264(19) Å respectively [17, 18]. It could be viewed, however, that the Pd1-N1 bond distance in the complex is shorter than the others suggesting the great interaction between the nitrogen atom and the empty d-orbital of Pd(II) metal. The crystal structure of this complex (see, Table 2) is stabilized by intramolecular N4-H4...S1 and C32-H32...C11 hydrogen bonds [19, 20].

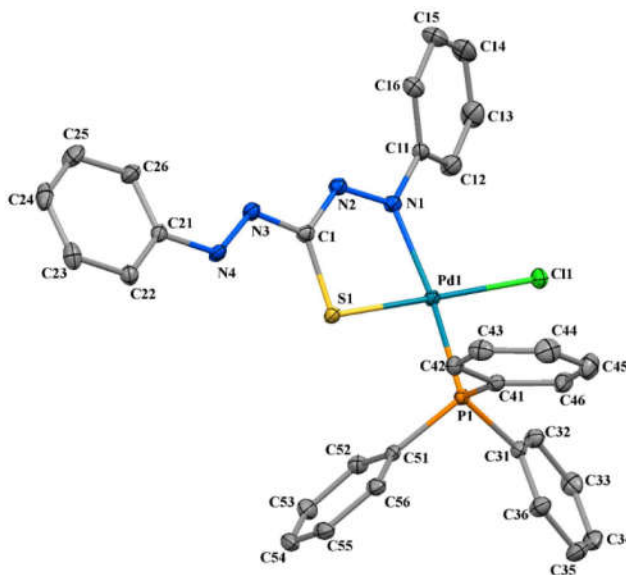


Figure 1. Crystal structure of [Pd(HDZ)(PPh<sub>3</sub>)Cl] shown at 30% ellipsoid probability, H atoms are omitted for clarity.

Table 2. Selected bond distances, bond angles, and Hydrogen bonds for the Pd(II) compound.

Bond	Distances, Å		Bond	Angle, °
Pd1-C11	2.3453(6)		C11-Pd1-S1	174.46(2)
Pd1-S1	2.2669(6)		C11-Pd1-P1	90.79(2)
Pd1-P1	2.2539(6)		C11-Pd1-N1	98.05(5)
Pd1-N1	2.1264(19)		S1-Pd1-P1	87.85(2)
N1-N2	1.282(3)		S1-Pd1-N1	82.65(5)
N3-N4	1.323(2)		P1-Pd1-N1	168.51(5)
P1-C31	1.823(2)		Pd1-N1-N2	120.27(13)
Hydrogen bonds for the Pd(II) complex; symmetry code: -X, 1/2+Y, 1/2-Z				
D-H...A	<i>d</i> (D-H) / Å	<i>d</i> (H...A) / Å	<i>d</i> (D...A) / Å	$\angle$ (DHA) / °
N4-H4...S1	0.83(2)	2.56(2)	2.930(2)	108.3(16)
C32-H32...C11	0.9500	2.7600	3.348(2)	121.00

Table 3. Energy properties (eV) and NBO Charge (e) of ligands and their Pd(II) complex.

Parameter	PPh <sub>3</sub>	Dithizone	Pd complex
HOMO	-5.531	-5.589	-3.685
LUMO	-0.642	-3.043	-3.041
$\Delta E$	4.889	2.546	0.644
Pd	-	-	-0.115
N1	-	-0.154	-0.087
N2	-	-0.313	-0.140
N3	-	-0.269	-0.282
N4	-	-0.338	-0.425
S	-	-0.209	-0.184
P1	0.806	-	0.781
C11	-	-	-0.156
C1	-	0.189	0.216

### Frontier orbitals

Frontier molecular orbitals are one of the most important theories for indicating molecular reactivity and stability. This theory predicts that a reaction between two chemical compounds is illustrated by the interaction between the HOMO orbital of one compound and the LUMO orbital of another compound [21]. The energy gap ( $E_{\text{HOMO}}-E_{\text{LUMO}}$ ) that splits the HOMO and LUMO orbitals are related to the reactivity and stability of chemical compounds. As we can see, a compound with a small HOMO-LUMO energy gap is more reactive than a compound with a big HOMO-LUMO energy gap. A compound with a wide HOMO-LUMO energy gap is more stable than a compound with a narrow HOMO-LUMO energy gap [22]. The theoretical values of the HOMO and LUMO orbitals of ligands and their palladium complex are shown in (Figure 2) and Table 3. In the free dithizone ligand, the energy gap between HOMO and LUMO orbitals is 2.546 eV while for triphenylphosphine is 4.889 eV [23]. We can see that the dithizone ligand is less stable and more reactive than the triphenylphosphine ligand. The value of the energy gap of the palladium complex is 0.644 eV. The energy gap values also imply that palladium complexes are less stable and more reactive than ligands [24].

### NBO atomic charges

Neutral bond orbital (NBO) studies were used to evaluate the delocalization of electron density between an electrophile atom (metal center) and nucleophile atoms (ligand donor atom), which is reciprocal to the charge stabilizing donor-acceptor interaction. Table 3 shows the natural charges

of ligands and the Pd(II) complex. The natural charge at the central atom for the Pd(II) complex was  $-0.115e$ , indicating that the ligands transfer a large amount of charge density to the palladium central metal [25]. The electron transport to the metal ion is confirmed by the net charges of donor atoms in Table 3. According to the method used in calculating the atomic charge, the sulfur atom S1 has a higher negative charge than the nitrogen N1 atom in the free ligand. This result indicates that sulfur S1 is more reactive to metallic attack than nitrogen N1, which is consistent with X-ray results indicating that the dithizone ligand is firmly coordinated to the metal ion via the sulfur atom [26].

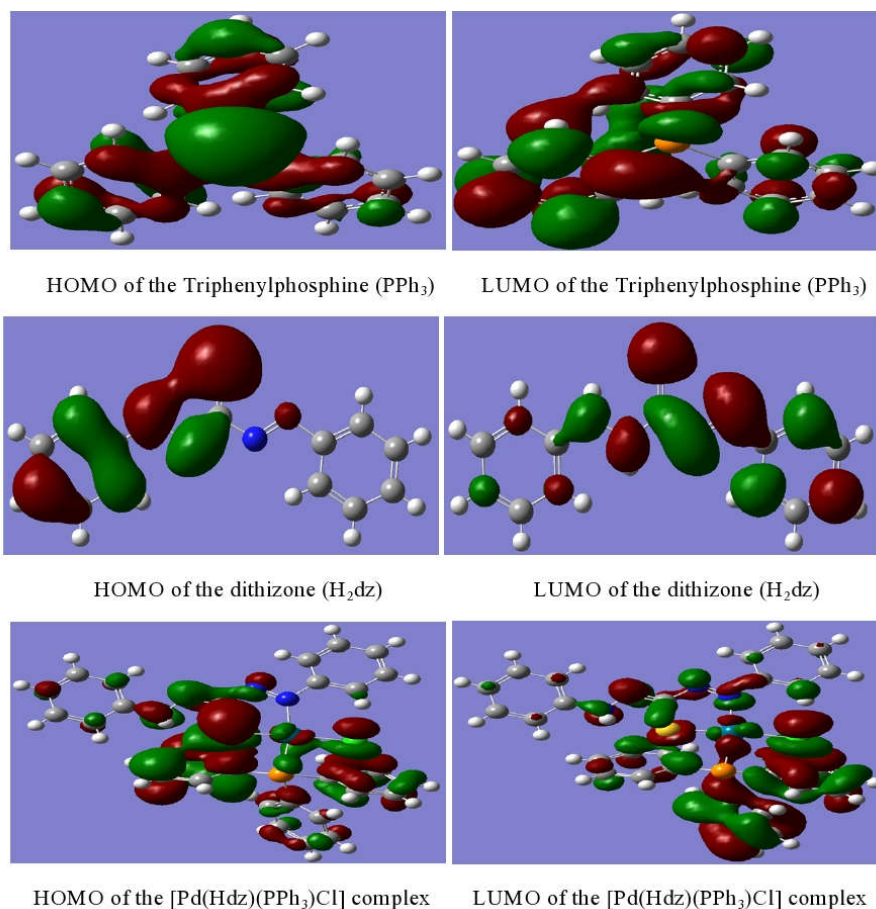


Figure 2. The illustrations of HOMO and LUMO orbitals of ligands and Pd(II) complex.

#### *Electronic spectra and conductivity properties*

The electronic spectra of the ligands and their Pd(II) complex are displayed in (Figure 3). The spectrum of free ligand  $\text{PPh}_3$  exhibits a band at  $37735 \text{ cm}^{-1}$  (265 nm), which is attributed to the  $\pi\text{-}\pi^*$  transition. This band shifts to  $37037 \text{ cm}^{-1}$  (270 nm) on complexation, revealing the connection of the phosphor atom to the Palladium ion [27]. The free dithizone ligand illustrates two bands. The first one come out at  $39379 \text{ cm}^{-1}$  (254 nm), which corresponded to the  $\pi\text{-}\pi^*$

transition. While, the other is broadband and appears in the visible region at  $24096\text{ cm}^{-1}$  (415 nm), which is related to the  $n-\pi^*$  electronic transition [28]. The absorption spectra of the Pd(II) complex showed two spin-allowed singlet-singlet d-d electronic transition bands at  $19083$  and  $28735\text{ cm}^{-1}$  (524 and 348 nm) and interrelated to  ${}^1B_{1g} \leftarrow {}^1A_{1g}$  and  ${}^1E_g \leftarrow {}^1A_{1g}$  transition, respectively. The band at  $32573\text{ cm}^{-1}$  (307 nm) is assigned to a combination of metal to ligand charge transfer (MLCT). According to electronic spectra, the Pd(II) complex is found to be distorted square planar geometry [29]. The molar conductivity value in DMSO ( $7.06 \times 10^{-5}\text{ S} \cdot \text{cm}^2 \cdot \text{mol}^{-1}$ ) of the prepared complex was found to be very low, implying that this is non-electrolyte in nature [30].

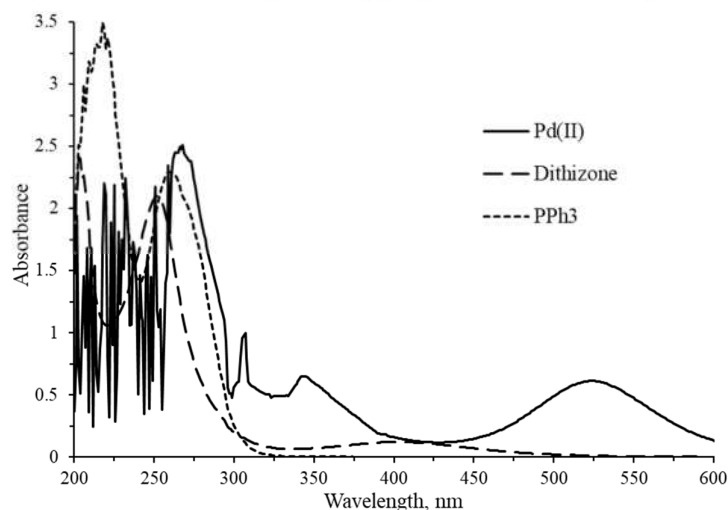


Figure 3. Electronic absorption spectra of ligands and Pd(II) complex.

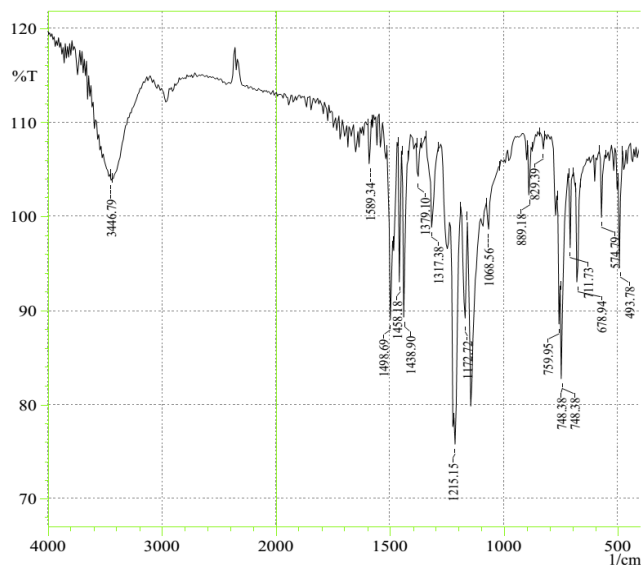


Figure 4. IR spectrum of dithizone ( $\text{H}_2\text{dz}$ ) ligand.

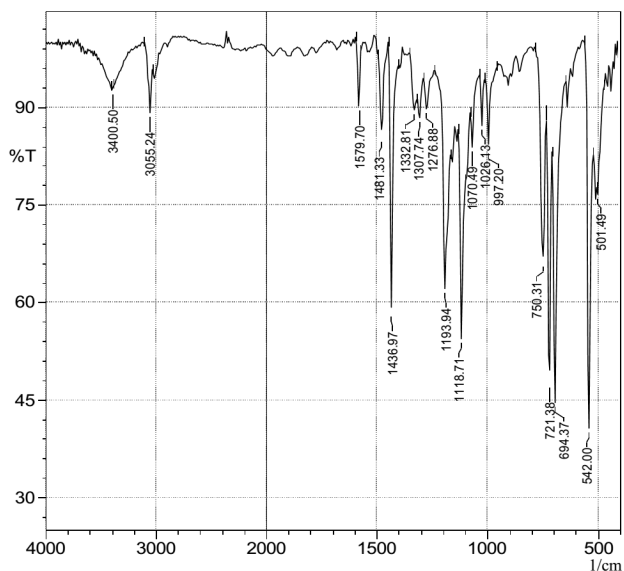


Figure 5. IR spectrum of  $[\text{Pd}(\text{Hdz})(\text{PPh}_3)\text{Cl}]$  complex.

#### FT-IR study

The IR spectrum of the dithizone ligand (Figure 4), showed broadband at  $3446\text{ cm}^{-1}$  was attributed to  $\nu(\text{N-H})$  stretching frequency [31]. A strong band at  $1579\text{ cm}^{-1}$  in the Pd(II) complex (Figure 5), indicating that the N atom coordinates with palladium metal [32]. The appearance of a new band at  $542\text{ cm}^{-1}$ , attributed to  $\nu(\text{Pd-N})$ , also confirms the coordination of the nitrogen atom to a metal center [33]. A weak band observed at  $759\text{ cm}^{-1}$ , assigned to  $\nu(\text{C-S})$  in the dithizone ligand, shifts to a lower frequency of  $750\text{ cm}^{-1}$ , which reinforces the coordination of the sulfur atom to the Pd(II) center [34]. The strong band was observed at  $1436\text{ cm}^{-1}$  related to  $\nu(\text{P-Ph})$  [35].

### CONCLUSION

To summarize, we have described the convenient synthesis and extensive identification of a novel palladium(II) complex containing dithizone and triphenylphosphine ligands. Based on the results of identification techniques, the dithizone and  $\text{PPh}_3$  ligands are ligated to the Pd(II) metal center in a distorted square planar geometry. The electronic spectra of the complex exhibited peaks at  $19083$  and  $28735\text{ cm}^{-1}$ , which corresponded to  ${}^1\text{B}_{1g} \leftarrow {}^1\text{A}_{1g}$  and  ${}^1\text{E}_g \leftarrow {}^1\text{A}_{1g}$  transitions, respectively. The NBO results reveal that Pd-X bond interaction energies can be related to the strong ligand to metal charge transfer and decreased by changing the X atom from N, P, S, and Cl. The DFT study reveals that the palladium complex was less stable and more reactive than ligands.

### ACKNOWLEDGMENTS

The authors are grateful to the University of Salahaddin and the University of Halabja for providing the required assistance to complete the present study. We acknowledge Nelson Mandela University for single-crystal X-ray diffraction analysis. Finally, we thank Mr. Mzgin Ayoob for assisting us with the FT-IR measurement.

## REFERENCES

1. Abdulnabi, Z.A.; Al-doghachi, F.A.J.; Abdulsahib, H.T. Synthesis, characterization and thermogravimetric study of some metal complexes of selenazone ligand nanoparticles analogue of dithizone. *Indones. J. Chem.* **2021**, *21*, 1231-1243.
2. Maghazy, M.A.; Moalla, S.M.N.; Rashed, M.N.; Abd El Aziz, A. Determination of Cd<sup>2+</sup>, Cu<sup>2+</sup>, Mn<sup>2+</sup>, Pb<sup>2+</sup>, and Zn<sup>2+</sup> in aqueous solution after their separation and preconcentration as metal-dithizone complexes on activated carbon. *Aswan Univ. J. Environ. Stud.* **2020**, *1*, 157-170.
3. Mudasir, M.; Karelius, K.; Aprilita, N.H.; Wahyuni, E.T. Adsorption of mercury(II) on dithizone-immobilized natural zeolite. *J. Environ. Chem. Eng.* **2016**, *4*, 1839-1849.
4. Gaál, A.; Orgován, G.; Mihucz, V.G.; Pape, I.; Ingerle, D.; Strelí, C.; Szoboszlai, N. Metal transport capabilities of anticancer copper chelators. *J. Trace Elem. Med. Biol.* **2018**, *47*, 79-88.
5. Rice, C.R.; Faulkner, R.A.; Jewsbury, R.A.; Bullock, S.; Dunmore, R. A structural study of dithizone coordination chemistry. *Cryst. Eng. Comm.* **2017**, *19*, 3414-3419.
6. Ntoi, L.L. *Multiple chromisms associated with dithizone*. PhD Thesis, Free State University, Bloemfontein, South Africa, **2016**.
7. Chiweshe, T.T.; Landman, M.; Conradie, J.; Von Eschwege, K.G. Synthesis and structure of dithizonato complexes of antimony(III), copper(II) and tin(IV). *J. Coord. Chem.* **2016**, *69*, 788-800.
8. Bakherad, M.; Jajarmi, S.A. dithizone-functionalized polystyrene resin-supported Pd(II) complex as an effective catalyst for Suzuki, Heck, and copper-free Sonogashira reactions under aerobic conditions in water. *J. Mol. Catal. A Chem.* **2013**, *370*, 152-159.
9. Delgado, J.A.; Okio, C.K.; Welter, R. Synthesis, characterization, crystal structure and theoretical calculations of an organotin(IV) complex with dithizone. *Inorg. Chem. Commun.* **2009**, *12*, 1074-1076.
10. Sheldrick, G.M. SHELXT—Integrated space-group and crystal-structure determination. *Acta Cryst. A* **2015**, *71*, 3-8.
11. Hübschle, C.B.; Sheldrick, G.M.; Dittrich, B. ShelXle: a Qt graphical user interface for SHELXL. *J. Appl. Crystallogr.* **2011**, *44*, 1281-1284.
12. Krause, L.; Herbst-Irmer, R.; Sheldrick, G.M.; Stalke, D. Comparison of silver and molybdenum microfocus X-ray sources for single-crystal structure determination. *J. Appl. Cryst.* **2015**, *48*, 3-10.
13. Zaater, S.; Bouchoucha, A.; Djebbar, S.; Brahimi, M. Structure, vibrational analysis, electronic properties and chemical reactivity of two benzoxazole derivatives: Functional density theory study. *J. Mol. Struct.* **2016**, *1123*, 344-354.
14. Tabrizi, L.; Dao, D.Q.; Vu, T.A. Experimental and theoretical evaluation on the antioxidant activity of a copper(II) complex based on lidocaine and ibuprofen amide-phenanthroline agents. *RSC Adv.* **2019**, *9*, 3320-3335.
15. Chen, S.L.; Liu, Z.; Liu, J.; Han, G.C.; Li, Y.H. Synthesis, characterization, crystal structure and theoretical approach of Cu(II) complex with 4- $\{(Z)-[(2\text{-hydroxybenzoyl})\text{hydrazone}]\text{methyl}\}$  benzoic acid. *J. Mol. Struct.* **2012**, *1014*, 110-118.
16. Kumar, P.R.; Upreti, S.; Singh, A.K. Schiff bases functionalized with PPh<sub>2</sub> and SPh groups and their Ni(II) and Pd(II) complexes: Synthesis, crystal structures and applications of a Pd complex for Suzuki–Miyaura coupling. *Polyhedron* **2008**, *27*, 1610-1622.
17. Tamizh, M.M.; Karvembu, R. Synthesis of triethylphosphite complexes of nickel(II) and palladium(II) with tridentate Schiff base ligand for catalytic application in carbon–carbon coupling reactions. *Inorg. Chem. Commun.* **2012**, *25*, 30-34.
18. Romm, I.P.; Malkov, A.A.; Lebedev, S.A.; Levashova, V.V.; Buslaeva, T.M. The electronic spectra and structure of palladium(II) molecular complexes and clusters. *Russ. J. Phys. Chem.* **2011**, *85*, 248-253.

19. Karami, K.; Sadeghi-Aliabadi, H.; Lipkowski, J.; Mirian, M. Dinuclear bridged biphosphinic and mononuclear cyclopalladated complexes of benzylamines: Synthesis, structural characterization, and antitumor activity. *Polyhedron* **2013**, *50*, 187-192.
20. Spackman, M.A.; McKinnon, J.J. Fingerprinting intermolecular interactions in molecular crystals. *Cryst. Eng. Comm.* **2002**, *4*, 378-392.
21. Choudhary, V.; Bhatt, A.; Dash, D.; Sharma, N. DFT calculations on molecular structures, HOMO–LUMO study, reactivity descriptors, and spectral analyses of newly synthesized diorganotin(IV) 2-chloridophenylacetohydroxamate complexes. *J. Comput. Chem.* **2019**, *40*, 2354-2363.
22. Balaban Gündüzalp, A.; Özbek, N.; Karacan, N. Synthesis, characterization, and antibacterial activity of the ligands including thiophene/furan ring systems and their Cu(II), Zn(II) complexes. *J. Med. Chem. Res.* **2012**, *21*, 3435-3444.
23. Allab, Y.; Chikhi, S.; Zaater, S.; Brahimi, M.; Djebbar, S. Impact of the functionalized tetrazole ring on the electrochemical behavior and biological activities of novel nickel(II) complexes with a series of tetrazole derivatives. *Inorg. Chem. Acta* **2020**, *504*, 119436.
24. Gaber, M.; Awad, M.K.; Atlam, F.M. Pd(II) complexes of bidentate chalcone ligands: Synthesis, spectral, thermal, antitumor, antioxidant, antimicrobial, DFT and SAR studies. *J. Mol. Struct.* **2018**, *1160*, 348-359.
25. Ghani, N.T.A.; Mansour, A.M. Novel palladium(II) and platinum(II) complexes with 1H-benzimidazol-2-ylmethyl-N-(4-bromo-phenyl)-amine: Structural studies and anticancer activity. *Eur. J. Med. Chem.* **2012**, *47*, 399-411.
26. Guelai, A.; Brahim, H.; Guendouzi, A.; Boumediene, M.; Brahim, S. Structure, electronic properties, and NBO and TD-DFT analyses of nickel(II), zinc(II), and palladium(II) complexes based on Schiff-base ligands. *J. Mol. Model.* **2018**, *24*, 1-12.
27. Reva, I.; Lapinski, L.; Nowak, M.J. Photoinduced oxidation of triphenylphosphine isolated in a low-temperature oxygen matrix. *Chem. Phys. Lett.* **2008**, *467*, 97-100.
28. Fu, J.; Wang, X.; Li, J.; Ding, Y.; Chen, L. Synthesis of multi-ion imprinted polymers based on dithizone chelation for simultaneous removal of Hg<sup>2+</sup>, Cd<sup>2+</sup>, Ni<sup>2+</sup> and Cu<sup>2+</sup> from aqueous solutions. *RSC Adv.* **2016**, *6*, 44087-44095.
29. Mishra, A.K.; Mishra, S.B.; Kaushik, N.K. Palladium(II) thiohydrazone complexes: synthesis, spectral characterization, and antifungal study. *J. Coord. Chem.* **2007**, *60*, 1691-1700.
30. El-Sherif, A.A. Synthesis and characterization of some potential antitumor palladium(II) complexes of 2-aminomethylbenzimidazole and amino acids. *J. Coord. Chem.* **2011**, *64*, 2035-2055.
31. Refat, M.S.; Altalhi, T.A.; Al-Hazmi, G.H.; Al-Humaidi, J.Y. Synthesis, characterization, thermal analysis and biological study of new thiophene derivative containing o-aminobenzoic acid ligand and its Mn(II), Cu(II) and Co(II) metal complexes. *Bull. Chem. Soc. Ethiop.* **2021**, *35*, 129-140.
32. Özdemir, Ü.Ö.; Akkaya, N.; Özbek, N. New nickel(II), palladium(II), platinum(II) complexes with aromatic methanesulfonylhydrazone based ligands. Synthesis, spectroscopic characterization and in vitro antibacterial evaluation. *Inorg. Chim. Acta* **2013**, *400*, 13-19.
33. Wang, S.; Shi, Y.; Shao, W.; Du, J.; Wei, H.; Zhang, J.; Wang, K.; Shen, S.; Li, S.; Li, J.; Zhao, Y. Synthesis, characterization and cytotoxicity of gold(III) complexes with deprotonated pyridyl carboxamide. *Appl. Organomet. Chem.* **2012**, *26*, 504-510.
34. Prabhakaran, R.; Renukadevi, S.V.; Karvembu, R.; Huang, R.; Mautz, J.; Huttner, G.; Subashkumar, R.; Natarajan, K. Structural and biological studies of mononuclear palladium (II) complexes containing N-substituted thiosemicarbazones. *Eur. J. Med. Chem.* **2008**, *43*, 268-273.
35. Bal-Demirci, T.; Güveli, Ş.; Yeşilyurt, S.; Özdemir, N.; Ülküseven, B. Thiosemicarbazone ligand, nickel(II) and ruthenium(II) complexes based on vitamin B6 vitamer: The synthesis, different coordination behaviors and antioxidant activities. *Inorg. Chim. Acta* **2020**, *502*, 119335.